Journal Of Phycology
December 2014, Volume 50 Issue 6 Pages 1120-1136
http://dx.doi.org/10.1111/jpy.12244
http://archimer.ifremer.fr/doc/00226/33678/

Ailadinium reticulatum gen. et sp. nov. (Dinophyceae), a New Thecate, Marine, Sand-Dwelling Dinoflagellate from the Northern Red Sea

Saburova Maria [1, *], Chomérat Nicolas [2]

[1] Inst Biol Southern Seas, UA-99011 Sevastopol, Ukraine.
[2] IFREMER, Stn Biol Marine, LER BO, F-29900 Concarneau, France.

* Corresponding author : Maria Saburova, email address : msaburova@gmail.com

Abstract :

A new photosynthetic, sand-dwelling marine dinoflagellate, *Ailadinium reticulatum* gen. et sp. nov., is described from the Jordanian coast in the Gulf of Aqaba, northern Red Sea, based on detailed morphological and molecular data. *A. reticulatum* is a large (53–61 µm long and 38–48 µm wide), dorsoventrally compressed species, with the epitheca smaller than the hypotheca. The theca of this new species is thick and peculiarly ornamented with round to polygonal depressions forming a foveate-reticulate thecal surface structure. The Kofoidian thecal tabulation is APC (Po, cp), 4′, 2a, 6″, 6c, 4s, 6‴, 1p, 1⁗ or alternatively it can be interpreted as APC, 4′, 2a, 6″, 6c, 4s, 6‴, 2⁗. The plate pattern of *A. reticulatum* is noticeably different from described dinoflagellate genera. Phylogenetic analyses based on the SSU and LSU rDNA genes did not show any supported affinities with currently known thecate dinoflagellates.

Keywords : benthic dinoflagellates, Dinophyceae, Gulf of Aqaba, Jordan, LSU rDNA, molecular phylogeny, morphology, Red Sea, SSU rDNA, taxonomy

INTRODUCTION

In recent decades, it has been shown that marine bottom sediments are inhabited by diverse and abundant assemblage of dinoflagellates (e.g. Balech 1956; Fukuyo 1981; Larsen 1985; Hoppenrath 2000a; Faust et al. 2005; Murray 2009; Saburova et al. 2009). Among them, many new taxa with unusual plate patterns have been found and described (e.g. Nie and Wang 1944; Faust and Balech 1993; Horiguchi 1995; Murray and Patterson 2004; Hoppenrath and Selina 2006; Murray et al. 2006; Chomérat and Nézan 2009; Chomérat et al. 2010a; Nézan and Chomérat 2011), but benthic dinoflagellates remain still poorly investigated compared to planktonic species.

The relatively short Jordanian coast of the northern Red Sea (the Gulf of Aqaba) is known for its well-developed inshore coral reefs that provide a perfect habitat for biota and support abundant and diverse communities of coral fish and benthic invertebrates (UNEP/IUCN 1988). Studies of this marine ecosystem have been focused more on macrobenthic communities (e.g. Ismail 1986; Al-Zibdah et al. 2007), while yet little information exists on microbenthic organisms, despite their probable importance in supplying the next trophic levels. Very recently, benthic dinoflagellate assemblages have been preliminarily described for the first time with emphasis on ciguatera-related species for the central Red Sea off the Saudi Arabia coast (Catania 2012), and from the northern Red Sea (Saburova et al. 2013); however, there is considerable diversity yet to be described in sand-dwelling dinoflagellates of this region.

During preliminary taxonomic surveys of the benthic dinoflagellates inhabiting the bottom sandy sediments within inshore coral reef at Jordanian coast in the northern Red Sea, we have recorded a large-sized photosynthetic sand-dwelling dinoflagellate with unique features that cannot be associated with any currently described species or genus. The present paper describes this taxon on the basis of light and electron microscopical observations and phylogenetic rDNA study.

MATERIALS AND METHODS

Sampling

Samples were collected at Jordanian coast in the northern Red Sea in the Gulf of Aqaba along the Aqaba Marine Park zone. The Jordanian coastline has a length of about 27 km with a discontinuous series of fringing reefs of 13 km length, interrupted by bays, which are mostly covered with seagrass meadows (UNEP/IUCN 1988). The average monthly seawater temperature of the Gulf of Aqaba ranges from 21ºC during February–March to about 26ºC in August–September with the seasonal amplitude of about 5.5ºC. The average value of salinity is close to 40.6 (Al-Rousan et al. 2007).

During the course of sampling in the Aqaba Marine Park at 29º25′58″ N, 34º58′26″ E, a total of 22 samples of the bottom sediments were collected on 24 October 2009, 29 and 30 October 2010, and 30 October 2011. Samples were collected on the shallow slope of the inshore fringing coral reef, where carbonate sands dominated, at depths of 1.5–3 m during snorkeling. The upper layer of the sand was scraped to a depth 0.5-1 cm using 50 ml Falcon tubes by diver. The water temperatures ranged between 23-25ºC during sampling courses.

Sample processing

The sand-dwelling dinoflagellate cells were separated from the sandy sediment by extraction using the frozen seawater method (Uhlig 1964) with a 110 μm mesh size. The material was preliminary viewed alive with a Leica DMIL inverted microscope at 35× to 200× magnifications. Alternatively, one replicate of each sample was preserved by 4% Lugol's solution and utilized to examine by SEM or molecular analysis.

Cells of *Ailadinium reticulatum* were rarely observed, being found on just two sampling occasions in 2009 and 2011, and in one occasion only in 2010. Despite diligent searching in all collected samples, only 31 specimens were found and were available to us for both

morphological and molecular analysis. For this reason, culture studies of this species have not been carried out.

Light and scanning electron microscopy

For detailed observation, cells were isolated by micropipetting in preparation for high-magnification photomicroscopy, and were examined with the Leica DMLM (Leica, Wetzlar, Germany) microscope at 630× to 1000× magnification. LM observation of the thecal plate tabulation was performed on cells stained with Calcofluor White M2R (Sigma Chemical Co.) according to the method of Fritz and Triemer (1985). To visualize nuclei, 4′,6-diamidino-2-phenylindole (DAPI) fluorochrome was applied to cells fixed in 2.5% glutaraldehyde. Micrographs were obtained using Leica DMLM microscope equipped with epifluorescence (100 W short arc mercury lamp), DIC optics, and Leica DFC 320 digital camera.

SEM was employed for detailed observations of the thecal surface. For SEM, cells were individually isolated and concentrated in 0.2 mL tubes containing distilled water and a drop of formaldehyde to prevent fungal development. Cells were filtered using polycarbonate membrane filters (Millipore RTTP Isopore, 1.2 μm pore size, Millipore, Billerica, MA, USA), rinsed in deionized water, and prepared according to Chomérat and Couté (2008). The examination was performed using a Quanta 200 (FEI, Eindhoven, the Netherlands) scanning electron microscope with an electron acceleration of 5 kV. The SEM photographs were presented on a uniform background using Adobe Photoshop CS2, v. 9.0.2 (Adobe Systems, San Jose, CA, USA).

Morphometric measurements were made either from the calibrated digital LM images using Leica Application Suite v. 3.7 software (Leica Microsystems Ltd, Switzerland) or were calculated from scanning electron micrographs. Cell dimensions were measured in 12 specimens. Dimensions are given as the mean ± standard deviation.

112 *Morphological description and taxonomic assignment*

113 To describe the thecal plate tabulation, the nomenclature of Kofoid (1909, 1911) was applied,
114 and the alternative plate pattern interpretation follows Balech (1980, 1988). The nomenclature of
115 Dodge and Hermes (1981) was applied for description of the apical pore complex. The general
116 dinoflagellate classification scheme proposed by Fensome et al. (1993) was adopted.

117

118 *DNA amplification and sequencing*

119 Single cells were isolated from samples with a capillary pipette under an Olympus IX41 inverted
120 microscope (Olympus, Tokyo). They were rinsed in several drops of distilled water and then
121 placed in a 0.2 mL PCR tube containing 5 µl of distilled water. Then, the tubes were stored at -
122 20°C prior to analysis. For PCR, tubes were thawed and processed as described previously in
123 Chomérat et al. (2010b, 2012).

124

125 *Phylogenetic analyses*

126 The SSU sequences obtained were aligned with other dinoflagellates sequences and other
127 Alveolates as external group, using MAFFT software version 7 (Katoh and Standley 2013) with
128 selection of the Q-INS-i algorithm which considers the secondary structure for the alignment.
129 The alignments were then refined by eye with MEGA software version 5.2.1 (Tamura et al.
130 2011). For SSU a dataset of 77 taxa, including a sequence of *Perkinsus marinus* as outgroup, and
131 1691 aligned positions has been used. For LSU, ambiguous parts of the alignment (including the
132 D2 domain) were excluded from the analysis using Gblocks software version 0.91b (Castresana
133 2000), with less stringent parameters. As a result a matrix of 52 taxa including three Ciliates
134 sequences as outgroups, and 812 positions was used. GenBank accession numbers of all
135 sequences used are available in the supplementary material (Appendix S1).

136 For each data set, evolutionary models were examined using maximum likelihood and
137 Bayesian Inference analysis. The evolutionary model was selected using jModelTest version

0.1.1 (Posada 2008). According to Akaike information criterion (AIC) and Bayesian information criterion (BIC), a general time reversible (GTR) model with a gamma correction (Γ) for among-site rate variation and invariant sites was chosen for the SSU dataset while a GTR model with no invariant sites was chosen for the LSU dataset.

Maximum likelihood analyses were performed using PhyML version 3.0 (Guindon et al. 2010), and Bayesian analyses were run using Mr Bayes version 3.1.2 (Ronquist and Huelsenbeck 2003). Bootstrap analysis (1000 pseudoreplicates) was used to assess the relative robustness of branches of the ML tree. Initial Bayesian analyses were run with a GTR model (nst=6) with rates set to invgamma (gamma for LSU dataset). Each analysis was performed using four Markov chains (MCMC), with two millions cycles for each chain. Trees were saved every 100 cycles and the first 2000 trees were discarded. Therefore, a majority-rule consensus tree was created from the remaining 18000 trees in order to examine the posterior probabilities of each clade. The best ML phylograms are shown with robustness values for each node (ML/BI).

RESULTS

Observations

Ailadinium Saburova et Chomérat gen. nov. (Figs. 1-6)

Descriptio: Genus repositum in Dinophyta, incertum ordinem et incertam familam; solitarium; marinum; cum theca, photosynthetica et in arena vivens. Thecae laminarum tabulatio APC (Po, cp), 4′, 2a, 6″, 6c, 4s, 6‴, 1p, 1⁗. Epitheca deminuta. Cellulae dorsoventraliter compressae. Thecae laminae valde reticulatae.

Genus of the phylum Dinophyta, order and family uncertain; solitary; marine; with a theca; photosynthetic and sand-dwelling. Plate formula: APC (Po, cp), 4′, 2a, 6″, 6c, 4s, 6‴, 1p, 1⁗.

Epitheca much smaller than hypotheca, cell dorsoventrally compressed. Highly ornamented reticulate theca.

Etymology: Referring to the ancient Greek name for Aqaba, 'Aila' (Parker 1997), where the dinoflagellate was discovered.

Type species: *Ailadinium reticulatum* Saburova et Chomérat sp. nov.

Ailadinium reticulatum Saburova et Chomérat sp. nov. (Figs. 1-6)

Descriptio: Generis proprietates. Cellulae ovatae dorsoventraliter complanatae et cum asymetrico hypothecae postico extremo. Longitudo: 53-61µm; latitudo: 38-48 µm; dorsoventralis altitudo 12.5-16.2 µm. Epitheca deminuta et leviter minus angusta quam hypotheca. Cingulum supraequatorium et ascendens circa sui latitudine. Sulcus antapicem attingens. Thecae superficies valde reticulata cum circularibus vel polygoniis depressionibus. Chloroplasti lutei-brunnei. Nucleus in hypothecae postica dimidia pars positus.

Characters as for the genus. Cells ovate, dorsoventrally compressed, with asymmetrically outlined posterior end, 53-61µm long, 38-48 µm wide, and 12.5-16.2 µm deep. Epitheca slightly narrower and much smaller than hypotheca. Cingulum premedian, ascending, displaced by about a cingular width. Sulcus reaching antapex. Thecal surface strongly ornamented with round to polygonal depressions. Chloroplasts golden-brown. Nucleus in lower half of hyposome.

Habitat: Marine, sand-dwelling.

Holotype: Fig. 3, a-f; SEM stub # CEDiT2014H35 stored at the CEDiT (Centre of Excellence for Dinophyte Taxonomy) dinoflagellate type collection, Wilhelmshaven, Germany.

Type locality: bottom sediments within shallow coral reef in the Aqaba Marine Park (29º25′58″ N, 34º58′26″ E), the Gulf of Aqaba, northern Red Sea, Jordan.

Etymology: The specific epithet refers to the reticulate structure of the thecal surface, forming polygonal depressions.

The cells are roughly ovate in ventral view and dorsoventrally compressed, with concave ventral side and convex dorsal one (Figs. 1, a-e; 3, a-f). The cells are 53-61 µm long (55.1±2.4, n=12), 38-48 µm wide (42.1±2.9, n=11), and 12.5-16.2 µm deep (14.9±2.1, n=3), with a length:width ratio of 1.24-1.39. The epitheca appears cap-shaped, pointed ventrally and rounded dorsally, much smaller and slightly narrower than the hypotheca (Figs. 1, a-f; 2, b, c and d; 3, a, b and d; 4, a-d; 6, a and b). The hypotheca is large, almost rectangular, with convex lateral sides (Figs. 1, a-f; 3, a and b; 6, a and b). Cells are irregularly rounded posteriorly, with strongly asymmetrical notched posterior part of the left lateral side (Fig. 1, a-c; 6, a and b). A single, small, claw-shaped antapical spine is located asymmetrically at the right side of the cell (Figs. 1a; 3, a and b; 5g). The cingulum is deeply incised, about 3.2-3.5 µm wide. It is slightly ascending with a displacement of about its own width on the ventral side, and horizontal on the dorsal side of the cell (Figs. 1, a-e; 2, a and b; 3, a-d; 4, a-d; 6, a and b). The sulcus extends from the cingulum to the antapex and is wider posteriorly (Figs. 1, a and e; 2, a and g; 3, a, d and e; 5a; 6a). The nucleus is spherical and located in the posterior part of the cell just below the middle of hypotheca (Fig. 1, g-i). Thecal plates are thick and remarkably reticulated, which is clearly visible under light microscope (Fig. 1, e and f). The cells contain deeply lobed golden-brown chloroplasts (Fig. 1, a-d and j). There are four peripheral pyrenoids with a ring-like starch

sheaths located at the corners of the hypotheca (Fig. 1, d, e and g). The cytoplasm may also contain one or several large pusules and numerous colorless or colored small globules (Fig. 1, a-d). The transverse flagellum runs inside the cingulum completely around the cell (Fig. 1b). The longitudinal flagellum arises at the upper part of the sulcus, and is slightly longer than the cell length.

The Kofoidian plate formula is APC (Po, cp), 4′, 2a, 6″, 6c, 4s, 6‴, 1p, 1⁗. The epitheca consists of 14 plates, comprising two plates of the apical pore complex (Po, cp), four apical plates (1′-4′), two anterior intercalary plates (1a, 2a) and six precingular plates (1″-6″) (Fig. 2, c-f; 4; 6, a-c). The APC is formed by apical pore and cover plates and placed deeper with respect to the plates surrounding it (Figs. 2, c-f; 3d; 4). The outer apical pore plate (Po) is narrow, about 7.3-8.1 μm long, and dorsoventrally oriented. It is hook-shaped and bent toward the left side of the cell (Figs. 3d; 4, b, c and e; 6c). Alongside the inner border of the Po, there is a single row of rectangular depressions surrounding the cover plate (Fig. 4, d and e). The inner cover plate (cp) appears as a long, narrow and hook-shaped ridge that runs through the whole pore plate (Fig. 4, b, c and e; 6c). Its short curved end is located dorsally, curved toward the left side of the cell and ornamented with several small bulging folds (Fig. 4, b-d and f), whereas the long and narrow smooth end is lying ventrally (Fig. 4, a-c). The APC is enclosed by four apical plates that form a distinctive rim bordering the Po plate. This rim is well-developed on the dorsal side of the cell, but rather smoothed ventrally (Fig. 4). The first apical plate (1′) is irregularly shaped, polygonal and elongated. It has a deep asymmetrical notch in its upper part, into which the Po plate fits, whereas its posterior end is pointed and contacts the two sulcal plates Sa and Sd (Figs. 2, a, c and e; 3, a and d; 4, a and c). The second and fourth apical plates (2′ and 4′) are dorsoventrally elongated, crescent-shaped and encircle the Po plate on its left and right sides (Figs. 2, c-f; 4c). Owing to the prominent reticulate ornamentation of the thecal surface that obscure the sutures between small epithecal plates, they were hardly distinguished with SEM, but were revealed in calcofluor-stained cells. Thanks to the observation of the epithecal plate pattern with

240 epifluorescence microscopy, three small plates were identified in the dorsal side of the epitheca
241 (Fig. 2, d and f). The third apical plate (3′) is the smallest of the apical series, pentagonal and
242 located dorsally; it is adjoining with the Po plate between 2′ and 4′ plates, and bears only two
243 polygonal depressions (Figs. 2, d and f; 4, f and g). There are two small anterior intercalary
244 plates (1a and 2a), which are contiguous and located dorsally. The 1a plate is the smallest,
245 pentagonal, and contacts with 2′, 3′, 2a, 2″ and 3″. The 2a plate is hexagonal and
246 characteristically ornamented with several polygonal depressions partly or completely
247 surrounded by prominent crest-like rims. It contacts with 1a, 3′, 4′, 3″, 4″ and 5″ (Figs. 2, d and
248 f; 4, c, d, f and g). The precingular series consists of six plates (1″-6″), which are more or less
249 trapezoidal in shape. The first and sixth precingular plates are largest of the precingular series, lie
250 ventrally, and together with the first apical plate form the ventral part of the epitheca, while 2″-
251 5″ plates are located on the dorsal side of the epitheca (Figs. 2, c and d; 4, c and d).
252 The cingulum is wide, completely encircling the cell and consists of six plates (1c-6c).
253 The first, second and sixth cingular plates are large, while the other cingular plates are smaller
254 and roughly similar in size. The right side of the first cingular plate (1c) is deeply notched in the
255 upper part, into which the anterior sulcal plate fits (Figs. 2, a-d and g; 4, a-d).
256 The sulcus consists of four plates (Figs. 2, a and g; 3, d and e; 5a). The small anterior
257 sulcal plate (Sa) almost completely invades the upper right corner of the first cingular plate (1c)
258 and touches the end of the first apical plate (1′) on the left. The relatively large right sulcal plate
259 (Sd) is six-sided and elongated, with a convex left border and a concave right one. It partly
260 invades the epitheca and touches the end of the first apical plate (1′) on the right. The Sd plate
261 contacts the right end of the cingulum (6c), the 6″ plate and the 6‴ plate. The left sulcal plate
262 (Ss) is small, rectangular and located posterior to Sa touching the lower right side of the 1c, the
263 upper right side of the first postcingular plate (1‴) and the top of the posterior sulcal plate. The
264 posterior sulcal plate (Sp) is the largest of the sulcal series, occupying a considerable portion of
265 the sulcus. The Sp plate is long, five-sided, and wider toward the posterior and elongates from

266 the Sd and Ss to the antapex. Its lateral sides contact the first (1‴) and sixth (6‴) postcingular
267 plates, and its wide posterior end is in contact mainly with the first antapical plate (1⁗) and
268 partly with the posterior intercalary plate (1p). Flagella pore(s) are obscured from view and are
269 not identified.
270 The hypotheca consists of eight plates, comprising six postcingular plates (1‴-6‴), one
271 posterior intercalary plate (1p) and one antapical plate (1⁗) (alternative interpretation of the
272 hypothecal plate tabulation is discussed below). The large and oblong first (1‴) and sixth (6‴)
273 postcingular plates elongate along the sulcus, occupying nearly the entire ventral part of the
274 hypotheca (Figs. 2, a and g; 3, a, d and e; 5a; 6, a and d), whereas the other hypothecal plates are
275 located dorsally (Figs. 2b; 3, b, c and f; 6, b and d) and asymmetrically arranged. The 2‴ plate is
276 the longest of the postcingular series and lie dorsally along the left lateral side of the hypotheca.
277 The 3‴ plate is the largest of the postcingular series. It is asymmetrically shaped, five-sided, with
278 almost straight left lateral side and concave right one, into which the fourth postcingular plate
279 (4‴) fits. In contrast with the 2‴ and 3‴ plates that elongate through the whole hypotheca, the
280 4‴ and 5‴ plates are much shorter and extend one half of the whole way from the cingulum to
281 the antapex. The 4‴ plate is small, narrowly elongated and four-sided, with convex left lateral
282 side. The 5‴ plate is almost quadrate. There is one posterior intercalary plate (1p) that is located
283 dorsally in the right posterior half of the hypotheca (Figs. 2, a and b; 3, b, c, e and f; 6, a, b and
284 d). The 1p plate is large, six-sided, and contacts with 3‴, 4‴, 5‴ and 6‴ postcingular plates, with
285 antapical plate (1⁗), and with posterior sulcal plate (Sp). The 1p plate is ornamented with a
286 single short claw-shaped antapical spine (Figs. 3, a and b; 5g). Only one five-sided antapical
287 plate (1⁗) with concave ventral side is present (Figs. 2, a and b; 3, b, e and f; 5a; 6, a, b and d).
288 The thecal surface is highly and variously ornamented. Dorsal and ventral cell sides differ
289 in ornamentation, and some plates are peculiarly decorated. The thecal surface of the convex
290 dorsal side is reticulate, strongly ornamented with polygonal depressions (Figs. 3, b, c and f; 4, f
291 and g; 5, b, c and f; 6b). Dorsal polygonal depressions with diameter ranging between 0.48-1.6

292 µm (1.27±0.26 µm, n=24) are closely appressed, deep, with well-developed raised and
293 crenulated sides. Most of the depressions contain from 3 up to 15 small pores of different size
294 (ranging from 0.11 to 0.16 µm in diameter) at the bottom, however, there are depressions without
295 pores (Fig. 5, b, c and f-i). The 2a plate on the dorsal side of the epitheca bears several
296 depressions surrounded by prominent crest-like rims (Figs. 4, c-f; 5h). The thecal surface of the
297 ventral side is foveate, ornamented with randomly scattered depressions, which are connected by
298 incomplete ridges (Figs. 3, a and d; 5, a, d and e; 6a). Ventral depressions are shallower than
299 dorsal ones, with smooth sides, round to oval, with diameter ranging between 0.62-0.87 µm
300 (0.78±0.08 µm, n=14), containing 4-12 small pores at the bottom. There are 5-7 larger
301 depressions located ventrally near the cell margins (Figs. 2a; 5e; 6a). They are ovate, 1.0-2.2 µm
302 in diameter, perforated by 27-45 small pores forming a sieve-like bottom. The sulcal plates are
303 ornamented almost like other ventral thecal plates, but depressions are smaller and less densely
304 arranged, except for Sa plate, which is devoid of ornamentation at all (Figs. 2g; 3, a and d; 5a).
305 The cingular plates possess shallow depressions; however, they are less developed than those on
306 other plates (Fig. 4, a-d).
307 Sutures on the theca are often wide and transversely striated (Figs. 1f; 3; 4, c and d; 5, b-
308 d), but they are narrow and smooth in younger specimens (Fig. 4, b and f).
309
310 *Known distribution and occurrence: A. reticulatum* was recorded from two closely spaced
311 localities of the Jordanian coast (the Gulf of Aqaba, northern Red Sea) in carbonate coral sands.
312 This species occurred rarely, being found in three samples of 22 sediment samples collected at
313 different times. The species has been observed in very low cell densities in comparison with
314 many other sand-dwelling dinoflagellates at this sampling site.
315
316 *Swimming behavior:* Our observations of *A. reticulatum* at low magnification revealed that
317 normally live cells slowly swim close to the substrate surface ventral side down, in a relatively

straight course, occasionally changing direction. Being disturbed, the cell immediately presses itself to the bottom with its ventral side and stands still for several minutes.

Sequence analysis and molecular phylogeny

Two identical sequences of the SSU rDNA were independently acquired from two isolated cells of *Ailadinium reticulatum* collected in 2010 and 2011. Additionally, two identical sequences of the LSU rDNA were independently acquired from two isolated cells of *A. reticulatum* collected in 2011. Sequences were deposited to GenBank under the accession numbers KJ187034, KJ187035 (SSU) and KJ187036, KJ187037 (LSU).

In phylogenies inferred from SSU and LSU rDNA, sequences of *A. reticulatum* formed a fully supported clade among dinoflagellates. However, in both cases, the placement of this clade was unclear and not supported (Figs 7 and 8). Consequently, no clear relationships with *Ailadinium* and other genera can be ascertained from molecular data. In the SSU rDNA phylogeny, the clade of *A. reticulatum* branched as a sister clade to *Amphidiniella sedentaria* Horiguchi and *Pileidinium ciceropse* Tamura et Horiguchi but this position is not supported (Fig. 7). In the LSU rDNA phylogeny, the clade of *A. reticulatum* branched at the base of the Gonyaulacales clade but without statistical support (Fig. 8).

DISCUSSION

Alternative plate pattern interpretation

As with many other benthic dinoflagellates, which often possess an unusual plate pattern, the thecal tabulation of *Ailadinium reticulatum* is rather difficult to interpret, and an alternative pattern can be proposed. In particular, the hypothecal plate arrangement and the sulcal area can be interpreted differently than we have described previously.

To facilitate the further comparison between *A. reticulatum* and previously described taxa, Kofoidian system of plate tabulation (Kofoid 1909, 1911) was used initially for the

hypotheca. In terms of Kofoidian system, the large plate located dorsally in the right posterior half of the hypotheca is interpreted by us as posterior intercalary plate (1p) because of its rather lateral than antapical position, as in some gonyaulacoid genera (Fensome et al. 1993). However, following Balech's modification of the Kofoidian system, in which the posterior intercalary series is defined as 'those touching neither the cingulum nor the sulcus' (Balech 1980), the posterior intercalary plate 1p may be reassigned as an antapical plate because of its contact with posterior sulcal plate. The hypotheca then possesses two antapical plates, of which the second antapical plate 2′′′′ is homologues of the 1p. Alternatively, the hypothecal plate tabulation of *A. reticulatum* may be interpreted as 6′′′, 0p, 2′′′′.

A. reticulatum possesses a rather simple sulcal area including four sulcal plates that is peculiar among dinoflagellates. However, owing to the rather asymmetrical structure of the sulcus and an unclear position of the flagellar pore, the sulcal plate arrangement may be subjected to different interpretation. In fact, the only two large sulcal plates are clearly visible, whereas two smaller plates are almost obscured in view and arranged inside the pocket-like upper part of the sulcus being overlapped by the larger sulcal plates. One more peculiarity of the sulcal area in *A. reticulatum* is that there are two upper sulcal plates touching the epitheca, but only one of them also contacts the proximal end of the cingulum, namely Sa in our interpretation in agreement with Graham (1942). The second upper sulcal plate was interpreted here as the right sulcal plate (Sd) because of its somewhat right position as described in *Amphidiniopsis uroensis* Toriumi, Yoshimatsu et Dodge (Toriumi et al. 2002). However, given rather anterior location in contact with epitheca in both the upper sulcal plates, they may also be interpreted alternatively as the anterior sulcal complex composed of the larger right anterior sulcal plate Sad (Sd in our previous interpretation) and the smaller left anterior sulcal plate Sas (Sa in previous interpretation). We do not exclude the presence of one more sulcal plate inside the pocket-like upper part of the sulcus.

370 *Comparison of morphology with other genera/species*

371 Being observed under light microscopy, cells of *Ailadinium reticulatum* seem to be similar to
372 dorsoventrally compressed members of the genus *Amphidiniopsis* Wołoszyńska with respect to
373 overall cell shape, cell proportion, size and outline of epitheca, ascending cingulum and often
374 strong thecal ornamentation. The plate tabulation of *Ailadinium reticulatum* in Balech's system
375 (APC, 4′, 2a, 6″, 6c, 4s, 6‴, 2⁗) somewhat resembles the overall plate arrangement of
376 *Amphidiniopsis* described as APC, 3-4′, 1-3a, 6-8″, 3-8c, 3-5s, 5(6)‴, 2⁗ (Hoppenrath 2000a;
377 Toriumi et al. 2002; Hoppenrath et al. 2009). Precingular series of *A. cristata* Hoppenrath, *A.*
378 *korewalensis* Murray et Patterson, *A. pectinaria* Toriumi, Yoshimatu et Dodge and *A. uroensis*
379 Toriumi, Yoshimatu et Dodge consists of six plates (6″) as in *Ailadinium reticulatum*, but these
380 species differ in number and arrangement of the apical intercalary plates possessing one (in case
381 of *A. cristata*) or three (in *A. korewalensis*, *A. pectinaria* and *A. uroensis*) rather than two
382 intercalary plates. *A. aculeata* Hoppenrath, *A. hexagona* Yoshimatsu, Toriumi et Dodge, *A.*
383 *hirsuta* (Balech) Dodge and *A. konovalovae* Selina et Hoppenrath are all rather similar to
384 *Ailadinium reticulatum* in arrangement of the apical and intercalar series (4′, 2a), but they differ
385 in possessing seven rather than six precingular plates. Thus, none of these species exactly
386 matches the epithecal pattern of *Ailadinium reticulatum*. Moreover, *Amphidiniopsis* species
387 differ significantly from *Ailadinium reticulatum* in hypothecal plate pattern, possessing five
388 rather six postcingular plates and two symmetrically arranged dorsally antapical plates, as well as
389 in the morphology of APC, cingulum and sulcus. Finally, in contrast to photosynthetic
390 *Ailadinium reticulatum*, *Amphidiniopsis* species are all heterotrophic (Hoppenrath 2000a; Murray
391 and Patterson 2002; Toriumi et al. 2002; Hoppenrath et al. 2009; Selina and Hoppenrath 2013).

392 The species most closely morphologically related to *Ailadinium reticulatum* by the plate
393 pattern is the small, scanty ornamented sand-dwelling *Amphidiniella sedentaria*, the type species
394 of the monotypic genus (Horiguchi 1995). Despite the conspicuous difference in the cell size and
395 thecal ornamentation, both species are sand-dwelling, photosynthetic, with similar shape, small

396 epitheca and large hypotheca. In both species, the cells are dorsoventrally compressed and
397 possess the ascending cingulum, widened posteriorly sulcus, and pyrenoid(s). *Ailadinium*
398 *reticulatum* has a plate tabulation interpreted in Balech's system, 4′, 2a, 6″, 6c, 4s, 6‴, 2⁗,
399 notably similar to that of *A. sedentaria* (4′, 1a, 7″, 5c, 4s, 6‴, 2⁗). The epithecal plate
400 arrangement is rather similar for both species in respect of the total number of the epithecal
401 plates and their pattern. Like to *Ailadinium reticulatum*, *A. sedentaria* possesses four apical
402 plates, of which the 1′ is asymmetrical and notched at its upper part, and 3′ is the smallest of the
403 series. Both species have peculiarly ornamented dorsally located anterior intercalary plate, but
404 differ from each other in the total number of plates in the intercalary and precingular series: *A.*
405 *sedentaria* has only one relatively large anterior intercalary plate and seven rather six precingular
406 plates. *Ailadinium reticulatum* differs from *A. sedentaria* in lacking of the ventral pore. Both
407 species have a rather similar composition of the apical pore complex consisted of the apical pore
408 plate with slit-like apical pore and the cover plate, but *A. sedentaria* has a bean-shaped Po
409 compared with narrowly elongated hook-shaped APC in *Ailadinium reticulatum*. Both species
410 have the same plate arrangement in the hypotheca that is conventionaly considered as most
411 conservative diagnostic feature in thecate dinoflagellates (Fensome et al. 1993).
412 Reticulated thecal morphology is a rather frequent character among both planktonic and
413 benthic dinoflagellates. Similar to *Ailadinium*, a highly foveate-reticulate ornamentation has been
414 described in some species of the genus *Sinophysis* Nie & Wang, including *S. canaliculata* Quod,
415 Ten-Hage, Turquet, Mascarell & Couté and *S. microcephala* Nie & Wang (Nie and Wang 1944;
416 Quod et al. 1999). The similar thecal ornamentation has been reported in benthic dinoflagellates
417 *Pileidinium ciceropse*, *Roscoffia capitata* Balech, *Cabra reticulata* Chomérat et Nézan,
418 *Thecadinium arenarium* Yoshimatsu, Tourimi et Dodge (Hoppenrath and Elbrächter 1998;
419 Yoshimatsu et al. 2004; Tamura and Horiguchi 2005; Chomérat and Nézan 2009), in some of
420 benthic *Prorocentrum* Ehrenberg (e.g. Hoppenrath et al. 2013), as well as in a number of
421 plankton dinoflagellates of the genera *Dinophysis* Ehrenberg, *Gonyaulax* Diesing, *Heterodinium*

Kofoid, *Protoceratium* Bergh and others (e.g. Kofoid 1906, 1911; Kofoid and Michener 1911; Röder et al. 2012). Most of species with highly reticulate theca are ornamented with more or less deep polygonal depressions possessing typically a single central pore, whereas the reticulations of *A. reticulatum* are unusually perforated with numerous very small pores at the bottom. Among the sand-dwelling species, *Thecadinium yashimaense* Yoshimatsu, Toriumi et Dodge (syn. *T. mucosum* Hoppenrath et Taylor; *T. foveolatum* Bolch) is the only species possessing the similar type of depressions that were described as large round openings having 4-10 small pores at the bottom (Hoppenrath et al. 2004). Additionally, newly described benthic dinoflagellate *Madanidium loirii* Chomérat possesses an area closely arranged small pores at the bottom of shallow depressions (Chomérat and Bilien 2014). Some benthic *Prorocentrum* species possess the special features on their thecal surface. *P. panamense* Grzebyk, Sako et Berland and *P. pseudopanamense* Chomérat et Nézan have a single large roundish depression with sieve-like bottom perforated by numerous small pores (Grzebyk et al. 1998; Chomérat et al. 2011). Moreover, the pair of large pores at the lower dorsal side in *Adenoides eludens* (Herdman) Balech contains the similar sieve-plates (Hoppenrath et al. 2003, 2013). The marginal depressions of *P. consutum* Chomérat et Nézan and *Pileidinium ciceropse* contain 3-4 small pores (Tamura and Horiguchi 2005; Mohammad-Noor et al. 2007; Chomérat et al. 2010b).

The possible involvement of these specific features with sieve-like bottom into the mucus excretion has been hypothesized in *T. yashimaense* (Hoppenrath et al. 2004) and may be supported by our recent observations. Probably, the marginal large depressions with numerous pores at the bottom that were found on the thecal surface in *A. reticulatum* could provide the momentary discharge of mucus supporting the rapid and durable attachment of cell to the substrate. A similar manner of connection with substrate has been found recently in cells of *P. panamense* that were commonly observed in culture as attached to the bottom at their antapical ends with mucus secreted from the small pores in the roundish depression with sieve-like bottom on the right valve (unpublished observation of the first author).

448 The most unusual feature of the epithecal structure in *A. reticulatum* is a peculiar shape of
449 the apical pore complex. The composition of the APC in *A. reticulatum* resembles that of
450 gonyaulacoids in which a canal plate (X) is absent (Fensome et al. 1993; Steidinger and Tangen
451 1996). The asymmetrical shape of the pore plate and presence of the cover plate covering the
452 apical pore is similar to that observed in members of the family Goniodomataceae Lindermann
453 such as *Alexandrium* Halim, *Goniodoma* Stein and *Pyrodinium* Plate (e.g. Dodge and Hermes
454 1981; Steidinger and Tangen, 1996), but the APC of *A. reticulatum* differs from all these taxa in
455 having a more narrow and elongated outline. This unusual strongly elongated shape reminds that
456 of some members in the peridinioid family Podolampaceae Lindermann such as *Gaarderia*,
457 *Heterobractum* and *Mysticella* Carbonell-Moore (1994), but they all have a canal plate. Although
458 the apical pore in *A. reticulatum* is completely obscured by the cover plate, it seems to have the
459 same path as its covering plate, being long with hooked end. The hooked end of the apical pore
460 in *A. reticulatum* is bent towards the left cell side that is side-reversed to all other dinoflagellates
461 bearing hook-shaped apical pore including species belonging to the genus *Gambierdiscus* Adachi
462 and Fukuyo (e.g. Litaker et al. 2009), *Fragilidium* Balech ex Loeblich III (e.g. Balech 1959;
463 Nézan and Chomérat 2009) and some *Thecadinium* species, e.g. *T. inclinatum* Balech and *T.*
464 *kofoidii* (Herdman) Larsen (Hoppenrath 2000b; Yoshimatsu et al. 2004). From the APC
465 morphology, the most similar species to *A. reticulatum* is *Cabra aremorica* Chomérat, Couté et
466 Nézan that also has the unusual side-reversed hook in APC (Chomérat et al. 2010a).
467 One additional morphological peculiarity of *A. reticulatum* is the presence of a small
468 anterior intercalary plate (2a) that distinctively differs from the surrounding epithecal plates in its
469 ornamentation. The similar peculiarly decorated epithecal plates has been described in a few
470 sand-dwelling dinoflagellates including some of *Thecadinium* (*T. arenarium*, *T. ovum*, *T.*
471 *striatum* Yoshimatsu, Toriumi et Dodge, *T. yashimaense*), and *A. sedentaria* (Horiguchi 1995;
472 Hoppenrath et al. 2004; Yoshimatsu et al. 2004).

The most unusual feature of the hypothecal plate arrangement in *A. reticulatum* is a peculiar placement of the posterior intercalary or second antapical plate (1p or 2′′′′ depending on the interpretation) that is located dorsally in the right posterior half of the hypotheca. This contradicts the typical hypothecal plate pattern of gonyaulacaleans with usually ventrally located single posterior intercalary plate at the left side of the hypotheca (Fensome et al. 1993). Owing to its side-reversed position, this plate is homologues of the 2′′′′ in Balech's system. The dorsal placement of the posterior intercalary plate(s) is unusual among gonyaulacaleans and the only has been described previously in *Pyrophacus* Stein (e.g. Fensome et al. 1993), *Adenoides* Balech (Hoppenrath et al. 2003), and *Amphidiniella* Horiguchi (1995).

Phylogeny

Molecular analyses revealed that *Ailadinium reticulatum* forms a new clade within dinoflagellates which is not clearly related to any known genus. This result strongly supports the erection of the new genus *Ailadinium* that appears genetically distant from all other dinoflagellates and forms a new lineage. Moreover, this genus corresponds to a new dinoflagellate lineage which is, at the moment, not possible to assign in any particular family or order with the genetic markers used. Notwithstanding the absence of support in the LSU phylogeny, the analysis inferred from this gene suggests that it could be related to Gonyaulacales, but this result needs further confirmation.

The newly described herein genus *Ailadinium* joins a specific group of 'strange' thecate sand-dwelling dinoflagellates, which also includes *Adenoides*, *Amphidiniella*, *Cabra* Murray et Patterson, *Herdmania* Dodge, *Madanidinium* Chomérat et Bilien, *Pileidinium* Tamura et Horiguchi, *Plagiodinium* Faust et Balech, *Planodinium* Saunders et Dodge, *Pseudothecadinium* Hoppenrath et Selina, *Rhinodinium* Murray et al., *Roscoffia* Balech and *Sabulodinium* Saunders et Dodge. Interestingly, similar to *Ailadinium*, most of the listed genera are monotypic and rarely

499 recorded. Additionally, unusual thecal patterns found in these ‘strange’ dinoflagellates do not
500 provide clear evidences for their systematic position based on existing taxonomic criteria.
501 Moreover, because of scarcely available molecular data, their phylogenetic affinities within the
502 Dinophyceae are not always clearly determined (Hoppenrath et al. 2003; Tamura and Horiguchi
503 2005; Hoppenrath et al. 2007; Yamaguchi et al. 2011; Chomérat and Bilien 2014).
504 The resemblance between *Ailadinium reticulatum* and dorsoventrally compressed
505 *Amphidiniopsis* species has been shown as superficial. Based on morphology alone, the plate
506 pattern found in *Ailadinium reticulatum* has an affinity to the basic plate tabulation in the
507 Gonyaulacales (Fensome et al. 1993) with respect to its overall strongly asymmetry,
508 characteristically shaped first apical plate and APC, and possessing four apical, six pre- and
509 postcingular, one posterior intercalary and one antapical plates. Surprisingly, a minute benthic
510 dinoflagellate *Amphidiniella sedentaria* has been found to be most closely related to large and
511 heavily ornamented *Ailadinium reticulatum* by the similarity of shape, in the APC composition
512 and the total number of the epithecal plates, in possessing of small and peculiarly ornamented
513 apical intercalary plate, and in the same pattern of the hypothecal plates. However, *Ailadinium*
514 *reticulatum* and *Amphidiniella sedentaria* differ in the number of apical intercalary, precingular
515 and cingular plates and largely in size; therefore, we decided to consider them as members of
516 two different genera and to propose the erection of the new genus *Ailadinium*. Based on
517 morphological analysis, Horiguchi assigned the genus *Amphidiniella* to the Gonyaulacales
518 (Horiguchi 1995), however, this conclusion has not been supported by further phylogenetic study
519 (Tamura and Horiguchi 2005). Similarly, the affiliation of *Ailadinium* to the Gonyaulacales was
520 not supported in our phylogenetic analysis. For now, we can only conclude that *Ailadinium*
521 belongs to Peridiniphycideae incertae sedis and cannot be assigned to any existing supregeneric
522 taxa.
523
524

525 ACKNOWLEDGMENTS

526 We highly appreciate Dr. Igor Polikarpov (Kuwait Institute for Scientific Research, Kuwait)
527 valuable help with sampling and overall support during this work. We are grateful to anonymous
528 reviewers for their detailed and constructive comments. The authors wish to thank Mrs. G. Bilien
529 (IFREMER LER BO, France) for her assistance with the molecular work and Mr. N. Gayet
530 (REM/EEP/LEP IFREMER Brest Center, France) for his help with SEM. The authors are
531 grateful to Prof. Thomas S. Parker (North Carolina State University, USA) for his comments and
532 advice on the ancient Jordanian toponomy. This study was supported in part by the Foreign
533 Fellow Scientist Program at the French Research Institute for Exploitation of the Sea
534 (IFREMER, Concarneau, France).

535

536

537 REFERENCES

538 Al-Rousan, S., Felis, T., Manasrah, R. & Al-Horani, F. 2007. Seasonal variations in the stable
539 oxygen isotopic composition in *Porites* corals from the northern Gulf of Aqaba, Red Sea.
540 *Geochem. J.* 41:333–340.

541

542 Al-Zibdah, M. K., Damhoureyeh, S. A. & Badran, M. I. 2007. Temporal variations in coral reef
543 health at a coastal industrial site on the Gulf of Aqaba, Red Sea. *Oceanologia* 49(4):565–578.

544

545 Balech, E. 1956. Étude des dinoflagellés du sable de Roscoff. *Rev. Algol*. 2(1-2):29–52.

546

547 Balech, E. 1959. Two new genera of dinoflagellates from California. *Biol. Bull*. 116:195–203.

548

549 Balech, E. 1980. On thecal morphology of dinoflagellates with special emphasis on circular and
550 sulcal plates. *An. Centro Cienc. del Mar y Limnol. Univ. Nal. Auton. Mexico* 7(1):57–68.

551

552 Balech, E. 1988. Los dinoflagelados del atlantico sudoccidental. *Publ. Esp. Inst. Español*
553 *Oceanogr. Madrid* 1:1–310.

554

555 Carbonell-Moore, M. C. 1994. On the taxonomy of the family Podolampaceae Lindemann
556 (Dinophyceae) with descriptions of three new genera. *Rev. Paleobot. Palynol*. 84:73–99.

557

558 Catania, D. 2012. The prevalence of benthic dinoflagellates associated with ciguatera in the
559 Central Red Sea. MSc thesis. King Abdullah University of Science and Technology, Saudi
560 Arabia, 40 pp.

561

562 Chomérat, N. & Bilien, G. 2014. *Madanidinium loirii* gen. et sp. nov. (Dinophyceae), a new
563 marine benthic dinoflagellate from Martinique Island, Eastern Caribbean. *Eur. J. Phycol*.
564 49(2):165–178.

565

566 Chomérat, N. & Couté, A. 2008. *Protoperidinium bolmonense* sp. nov. (Peridiniales,
567 Dinophyceae), a small dinoflagellate from a brackish hypereutrophic lagoon (South of France).
568 *Phycologia* 47:392–403.

569

570 Chomérat, N., Couté, A. & Nézan, E. 2010a. Further investigations on the sand-dwelling genus
571 *Cabra* (Dinophyceae, Peridiniales) in South Brittany (northwestern France), including the
572 description of *C. aremorica* sp. nov. *Mar. Biodiv*. 40(2):131–142.

573

574 Chomérat, N. & Nézan, E. 2009. *Cabra reticulata* sp. nov. (Dinophyceae), a new sand-dwelling
575 dinoflagellate from the Atlantic Ocean. *Eur. J. Phycol*. 44:415–423.

576

577 Chomérat, N., Saburova, M., Bilien, G. & Al-Yamani, F. Y. 2012. *Prorocentrum bimaculatum*
578 sp. nov. (Dinophyceae, Prorocentrales), a new benthic dinoflagellate species from Kuwait
579 (Arabian Gulf). *J. Phycol.* 48:211–21.
580
581 Chomérat, N., Sellos, D. Y., Zentz, F. & Nézan, E. 2010b. Morphology and molecular phylogeny
582 of *Prorocentrum consutum* sp. nov. (Dinophyceae), a new benthic dinoflagellate from South
583 Brittany (northwestern France). *J. Phycol.* 46:183–94.
584
585 Chomérat, N., Zentz, F., Boulben, S., Bilien, G., van Wormhoudt, A. & Nézan, E. 2011.
586 *Prorocentrum glenanicum* sp. nov. and *Prorocentrum pseudopanamense* sp. nov.
587 (Prorocentrales, Dinophyceae), two new benthic dinoflagellate species from South Brittany
588 (northwestern France). *Phycologia* 50(2):202–214.
589
590 Dodge, J. D. & Hermes, H. B. 1981. A scanning electron microscopical study of the apical pores
591 of marine dinoflagellates (Dinophyceae). *Phycologia* 20(4):424–430.
592
593 Faust, M. A. & Balech, E. 1993. A further SEM study of marine benthic dinoflagellates from a
594 mangrove island, Twin Cays, Belize, including *Plagiodinium belizeanum* gen. et sp. nov. *J.*
595 *Phycol*. 29:826–832.
596
597 Faust, M. A., Litaker, R. W., Vandersea, M. W., Kibler, S. R. & Tester, P. A. 2005.
598 Dinoflagellate diversity and abundance in two Belizean coral-reef mangrove lagoons: a test of
599 Margalef's Mandala. *Atoll Research Bul*. 534:104–131.
600

601 Fensome, R. A., Taylor, F. J. R., Norris, D. R., Sargeant, W. A. S., Wharton, D. I. & Williams,
602 G. L. 1993. A classification of living and fossil dinoflagellates. *Micropaleontol. Spec. Publ*. 7:1–
603 351.
604
605 Fritz, L. & Triemer, R. E. 1985. A rapid simple technique utilizing calcofluor white MR2 for the
606 visualization of dinoflagellate thecal plates. *J. Phycol.* 21:662–664.
607
608 Fukuyo, Y. 1981. Taxonomical study on benthic dinoflagellates collected in coral reefs. *Bull.*
609 *Jap. Soc. Sci. Fish*. 47:967–978.
610
611 Graham, H. W. 1942. *Studies in the Morphology, Taxonomy, and Ecology of the Peridiniales*.
612 Carnegie Institution of Washington Publ. 542, Washington, 129 pp.
613
614 Grzebyk, D., Sako, Y. & Berland, B. 1998. Phylogenetic analysis of nine species of
615 *Prorocentrum* (Dinophyceae) inferred from 18S ribosomal DNA sequences, morphological
616 comparisons, and description of *Prorocentrum panamensis*, sp. nov. *J. Phycol*. 34:1055–1068.
617
618 Guindon, S., Dufayard, J.-F., Lefort, V., Anisimova, M., Hordijk, W. & Gascuel, O. 2010. New
619 algorithms and methods to estimate Maximum-Likelihood phylogenies: assessing the
620 performance of PhyML 3.0. *Syst. Biol.* 59:307–21.
621
622 Hoppenrath, M. 2000a. Taxonomische und ökologische Untersuchungen von Flagellaten mariner
623 Sande. Ph.D. dissertation, Biologische Fakultät, Universität Hamburg, Germany, 311 pp.
624

625 Hoppenrath, M. 2000b. Morphology and taxonomy of the marine sand-dwelling genus
626 *Thecadinium* (Dinophyceae), with the description of two new species from the North German
627 Wadden Sea. *Phycologia* 39:96–108.
628
629 Hoppenrath, M., Chomérat, N., Horiguchi, T., Schweikert, M., Nagahama, Y. & Murray S. 2013.
630 Taxonomy and phylogeny of the benthic *Prorocentrum* species (Dinophyceae) - a proposal and
631 review. *Harmful Algae* 27:1–28.
632
633 Hoppenrath, M. & Elbrächter, M. 1998. *Roscoffia capitata* (Dinophyceae) refound: notes on
634 morphology and biology. *Phycologia* 37:450–457.
635
636 Hoppenrath, M., Horiguchi, T., Miyoshi, Y., Selina, M., Taylor, F. J. R. & Leander, B. S. 2007.
637 Taxonomy, phylogeny, biogeography, and ecology of *Sabulodinium undulatum* (Dinophyceae),
638 including an emended description of the species. *Phycol. Res*. 55:159‑175.
639
640 Hoppenrath, M., Koeman, R. P. T. & Leander, B. S. 2009. Morphology and taxonomy of a new
641 marine sand-dwelling *Amphidiniopsis* species (Dinophyceae, Peridiniales), *A. aculeata* sp. nov.,
642 from Cap Feret, France. *Mar. Biodiv*. 39:1–7.
643
644 Hoppenrath, M., Saldarriaga, J. F., Schweikert, M., Elbrächter, M. & Taylor, F. J. R. 2004.
645 Description of *Thecadinium mucosum* sp. nov. (Dinophyceae), a new sand-dwelling marine
646 dinoflagellate, and an emended description of *Thecadinium inclinatum* Balech. *J. Phycol*.
647 40:946–61.
648

649 Hoppenrath, M., Schweikert, M. & Elbrächter M. 2003. Morphological reinvestigation and
650 characterization of the marine, sand-dwelling dinoflagellate *Adenoides eludens* (Dinophyceae).
651 *Eur. J. Phycol.* 38:385–394.
652
653 Hoppenrath, M. & Selina, M. 2006. *Pseudothecadinium campbellii* gen. nov. sp. nov.
654 (Dinophyceae), a phototrophic, thecate, marine planktonic species found in the Sea of Okhotsk,
655 Russia. *Phycologia* 45:260–269.
656
657 Horiguchi, T. 1995. *Amphidiniella sedentaria* gen. et sp. nov. (Dinophyceae), a new sand-
658 dwelling dinoflagellate from Japan. *Phycol. Res*. 43:93–99.
659
660 Ismail, N. S. 1986. Community structure of macrobenthic invertebrates in sandy beaches of the
661 Jordan, Gulf of Aqaba, Red Sea. *Int. Revue ges. Hydrobiol*. 71(2):225–232.
662
663 Katoh, K. & Standley, D. M. 2013. MAFFT multiple sequence alignment software version 7:
664 improvements in performance and usability. *Mol. Biol. Evol.* 30:772–80.
665
666 Kofoid, C. A. 1906. Dinoflagellata of the San Diego region. I. On *Heterodinium*, a new genus of
667 the Peridinidae. *Univ. Calif. Publ. Zool*. 2:341–368.
668
669 Kofoid, C. A. 1909. On *Peridinium steini* Jörgensen, with a note on the nomenclature of the
670 skeleton of the Peridinidae. *Arch. Protistenk*. 16:25–47.
671
672 Kofoid, C. A. 1911. Dinoflagellata of the San Diego region, IV. The genus *Gonyaulax*, with
673 notes on its skeletal morphology and a discussion of its generic and specific characters. *Univ.*
674 *Calif. Publ. Zool.* 8:187–286.

675

676 Kofoid, C. A. & Michener, J. R. 1911. New genera and species of dinoflagellates. No 22.
677 Reports on the Scientific Results of the Expedition to the Eastern Tropical Pacific in charge of
678 Alexander Agassiz, by the U. S. Fish Commission Steamer 'Albatross', from October, 1904, to
679 March, 1905, Lieut. Commander L. M. Garrett, U.S.N., commanding. *Bull. Mus. Comp. Zoöl.*
680 *Harvard College* 54:267–302.

681

682 Larsen, J. 1985. Algal studies of the Danish Wadden Sea II. A taxonomic study of psammobious
683 dinoflagellates. *Opera Bot*. 79:14–37.

684

685 Litaker R. W., Vandersea, M. W., Faust, M. A., Kibler, S. R., Chinain, M., Holmes, M. J.,
686 Holland, W. C. & Tester, P. A. 2009. Taxonomy of *Gambierdiscus* including four new species,
687 *Gambierdiscus caribaeus*, *Gambierdiscus carolinianus*, *Gambierdiscus carpenteri* and
688 *Gambierdiscus ruetzleri* (Gonyaulacales, Dinophyceae). *Phycologia* 48:344–390.

689

690 Mohammad-Noor, N., Daugbjerg, N., Moestrup, Ø. & Anton, A. 2007. Marine epibenthic
691 dinoflagellates from Malaysia – a study of live cultures and preserved samples based on light and
692 scanning electron microscopy. *Nord. J. Bot.* 24:629–690.

693

694 Murray, S. 2009. *Diversity and Phylogenetics of Sand-dwelling Dinoflagellates*. VDM Verlag
695 Dr. Müller Aktiengesellschaft & Co. KG, University of Sydney, Sydney, 213 pp.

696

697 Murray, S., Hoppenrath, M., Preisfeld, A., Larsen, J., Yoshimatsu, S.-A., Toriumi, S. &
698 Patterson, D. J. 2006. Phylogenetics of *Rhinodinium broomeense* gen. et sp. nov., a peridinioid,
699 sand dwelling dinoflagellate (Dinophyceae). *J. Phycol*. 42:934–942.

700

701 Murray, S. & Patterson, D. J. 2002. *Amphidiniopsis korewalensis* sp. nov., a new heterotrophic
702 benthic dinoflagellate. *Phycologia* 41:382–388.
703
704 Murray, S. & Patterson, D. J. 2004. *Cabra matta*, gen. nov., sp. nov., a new benthic,
705 heterotrophic dinoflagellate. *Eur. J. Phycol*. 39:229–234.
706
707 Nézan, E. & Chomérat, N. 2009. *Fragilidium duplocampanaeforme* sp. nov. (Dinophyceae): a
708 new phagotrophic dinoflagellate from the French Atlantic coast. *Eur. J. Protistol*. 45:2–12.
709
710 Nézan, E. & Chomérat, N. 2011. *Vulcanodinium rugosum* gen. et sp. nov. (Dinophyceae), un
711 nouveau dinoflagellé marin de la côte méditerranéenne française. *Cryptog. Algol*. 32(1):3–18.
712
713 Nie, D. & Wang, C.-C. 1944. Dinoflagellata of the Hainan Region. VIII. On *Sinophysis*
714 *microcephalus*, a new genus and species of Dinophysidae. *Sinensia* 15:145–151.
715
716 Parker, S. T. 1997. Preliminary report on the 1994 season of the Roman Aqaba Project. *Bull. Am.*
717 *Schools Orient. Res.* 305:19–44.
718
719 Posada, D. 2008. jModelTest: Phylogenetic model averaging. *Mol. Biol. Evol.* 25:1253–56.
720
721 Quod, J.-P., Ten-Hage, L., Turquet, J., Mascarell, G. & Couté A. 1999. *Sinophysis canaliculata*
722 sp. nov. (Dinophyceae), a new benthic dinoflagellate from western Indian Ocean islands.
723 *Phycologia* 38:87–91.
724
725 Röder, K., Hantzsche, F. M., Gebühr, C., Miene, C., Helbig, T., Krock, B., Hoppenrath, M.,
726 Luckas, B. & Gerdts, G. 2012. Effects of salinity, temperature and nutrients on growth, cellular

727 characteristics and yessotoxin oroduction of *Protoceratium reticulatum*. *Harmful Algae* 15:59–
728 70.
729
730 Ronquist, F. & Huelsenbeck, J. P. 2003. MrBayes 3: Bayesian phylogenetic inference under
731 mixed models. *Bioinformatics* 19:1572–74.
732
733 Saburova, M., Al-Yamani, F. & Polikarpov, I. 2009. Biodiversity of free-living flagellates in
734 Kuwait's intertidal sediments. *In* Krupp, F., Musselman, L. J., Kotb, M. M. A. & Weidig, I.
735 [Eds.] *Environment, Biodiversity and Conservation in the Middle-East*. Proceedings of the First
736 Middle Eastern Biodiversity Congress. Aqaba, Jordan, 20–23 October 2008. *Biorisk* 3:97–110.
737
738 Saburova, M., Polikarpov, I. & Al-Yamani, F. 2013. New records of the genus *Gambierdiscus* in
739 marginal seas of the Indian Ocean. *Mar. Biodiversity Rec*. 6(e91):1–11.
740
741 Selina, M. S. & Hoppenrath, M. 2013. Morphology and taxonomy of seven marine sand-
742 dwelling *Amphidiniopsis* species (Peridiniales, Dinophyceae), including two new species, *A.*
743 *konovalovae* sp. nov. and *A. striata* sp. nov., from the Sea of Japan, Russia. *Mar. Biodiv.* 43:87–
744 104.
745
746 Steidinger, K. A. & Tangen, K.1996. Dinoflagellates. *In* Tomas C. R. [Ed.] *Identifying Marine*
747 *Phytoplankton*. Academic Press, San Diego, pp. 387–584.
748
749 Tamura, M. & Horiguchi, T. 2005. *Pileidinium ciceropse* gen. et sp. nov. (Dinophyceae), a sand-
750 dwelling dinoflagellate from Palau. *Eur. J. Phycol*. 40:281–291.
751

752 Tamura, K., Peterson, D., Peterson, N., Stecher, G., Nei, M. & Kumar, S. 2011. MEGA5:
753 Molecular Evolutionary Genetics Analysis using Maximum Likelihood, evolutionary distance,
754 and Maximum Parsimony methods. *Mol. Biol. Evol.* 28:2731–39.
755
756 Toriumi, S., Yoshimatsu, S. & Dodge, J. D. 2002. *Amphidiniopsis uroensis* sp. nov. and
757 *Amphidiniopsis pectinaria* sp. nov. (Dinophyceae): two new benthic dinoflagellates from Japan.
758 *Phycol. Res*. 50:115–124.
759
760 Uhlig, G. 1964. Eine einfache Methode zur Extraktion der vagilen mesopsammalen Mikrofauna.
761 *Helgol. Wiss. Meeresunters*. 11:178–85.
762
763 UNEP/IUCN 1988. *Coral Reefs of the World. Volume 2: Indian Ocean, Red Sea and Gulf*.
764 UNEP Regional Seas Directories and Bibliographies. IUCN, Gland, Switzerland and Cambridge,
765 UK/UNEP, Nairobi, Kenya.
766
767 Yamaguchi, A., Hoppenrath, M., Pospelova, V., Horiguchi, T. and Leander, B. S. 2011.
768 Molecular phylogeny of the marine sand-dwelling dinoflagellate *Herdmania litoralis* and an
769 emended description of the closely related planktonic genus *Archaeperidinium* Jörgensen. *Eur. J.*
770 *Phycol*. 46:98–112.
771
772 Yoshimatsu, S., Toriumi, S. & Dodge, J. D. 2004. Morphology and taxonomy of five marine
773 sand-dwelling *Thecadinium* species Dinophyceae from Japan, including four new species
774 *Thecadinium arenarium* sp. nov., *Thecadinium ovatum* sp. nov., *Thecadinium striatum* sp. nov.
775 and *Thecadinium yashimaense* sp. nov. *Phycol. Res*. 52:211–223.
776
777

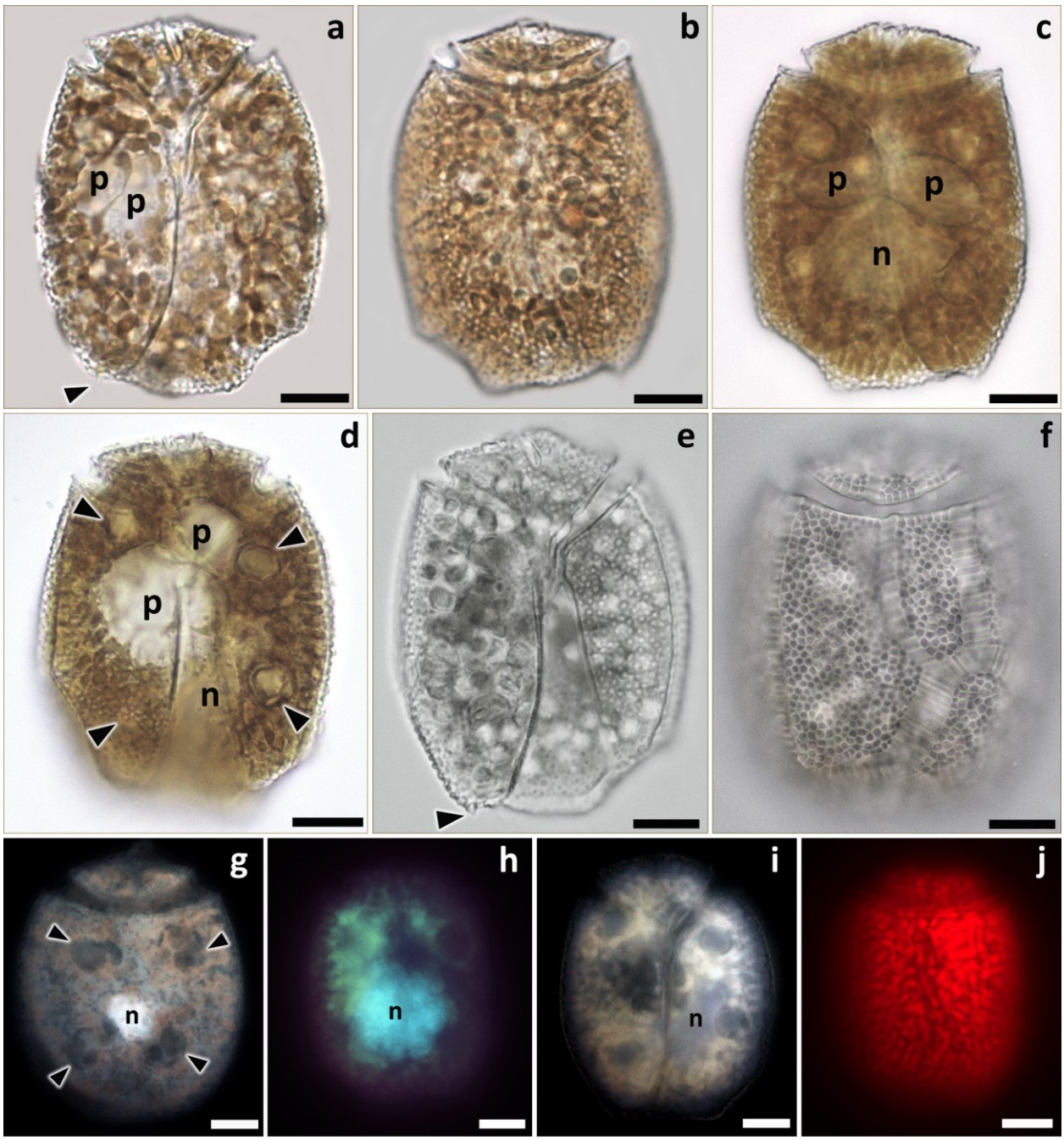

778

779 Fig. 1. Light micrographs of *Ailadinium reticulatum* gen. et sp. nov. from field samples. (a-d)
780 Bright field (BF) micrographs: (a) Ventral view, focus in the cell middle plane, showing
781 numerous chloroplasts, two small pusules (p) and asymmetrical antapical spine (arrowhead). (b)
782 Dorsal view, focus in the cell surface. Note the deeply indented cingulum and numerous colored
783 and colorless globules in the cytoplasm. (c, d) Dorsal view, focus in the cell middle plane,
784 showing numerous chloroplasts, pusules (p), nucleus (n) and four pyrenoids at the periphery of
785 the cell (arrowheads). (e, f) Differential interference contrast (DIC): (e) Ventral view showing
786 the thecal ornamentation and asymmetrical antapical spine (arrowhead). (f) Dorsal view showing
787 the thecal ornamentation. (g-i) Cells stained with DAPI and illuminated with UV light, showing
788 nucleus (n), arrowheads point pyrenoids. (j) Cell illuminated with UV light, showing the
789 chlorophyll autofluoresecence. Scale bar, 10 µm.
790

791

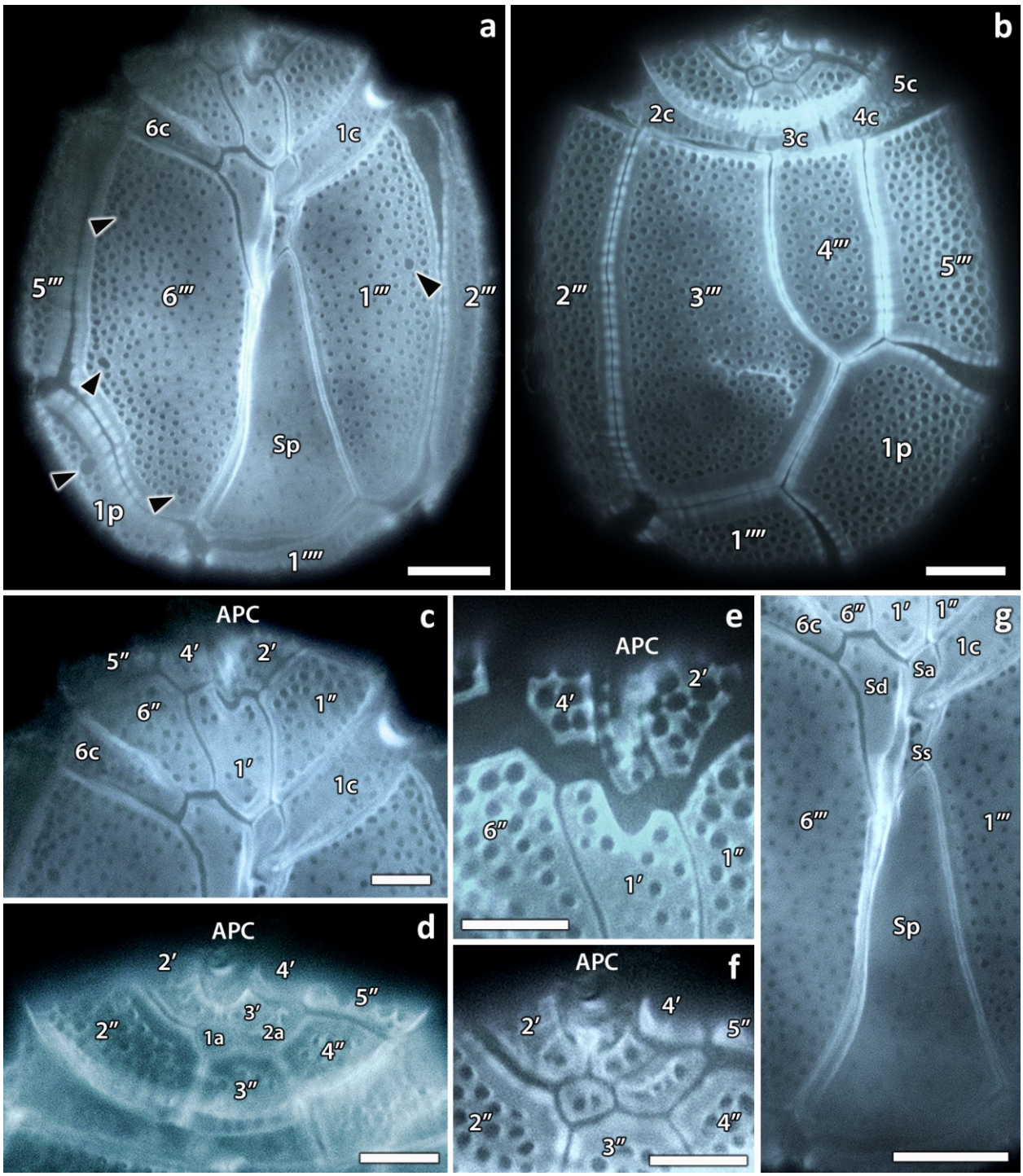

Fig. 2. Light micrographs of *Ailadinium reticulatum* gen. et sp. nov. (a-g) Cells stained with Calcofluor White and illuminated with UV light, showing the thecal plate pattern: (a) Ventral view of whole cell. Large marginal depressions are indicated by arrowheads. (b) Dorsal view of whole cell. (c) Detail of the ventral side of the epitheca. (d) Detail of the dorsal side of the epitheca. (e, f) APC and surrounded plates in ventral (e) and dorsal (f) views. (g) Detail of the sulcus with surrounded plates in ventral view. APC, apical pore complex; Po, apical pore plate; cp, cover plate; 1-4′, apical plate series; 1a-2a, anterior intercalary plates; 1-6″, precingular plate series; 1-6c, cingular plate series; 1-6‴, postcingular plate series; 1p, posterior intercalary plate; 1⁗, antapical plate; Sa, anterior sulcal plate; Sd, right sulcal plate; Ss, left sulcal plate; Sp, posterior sulcal plate. Scale bars, 10 μm in (a, b, g) and 5 μm in (c-f).

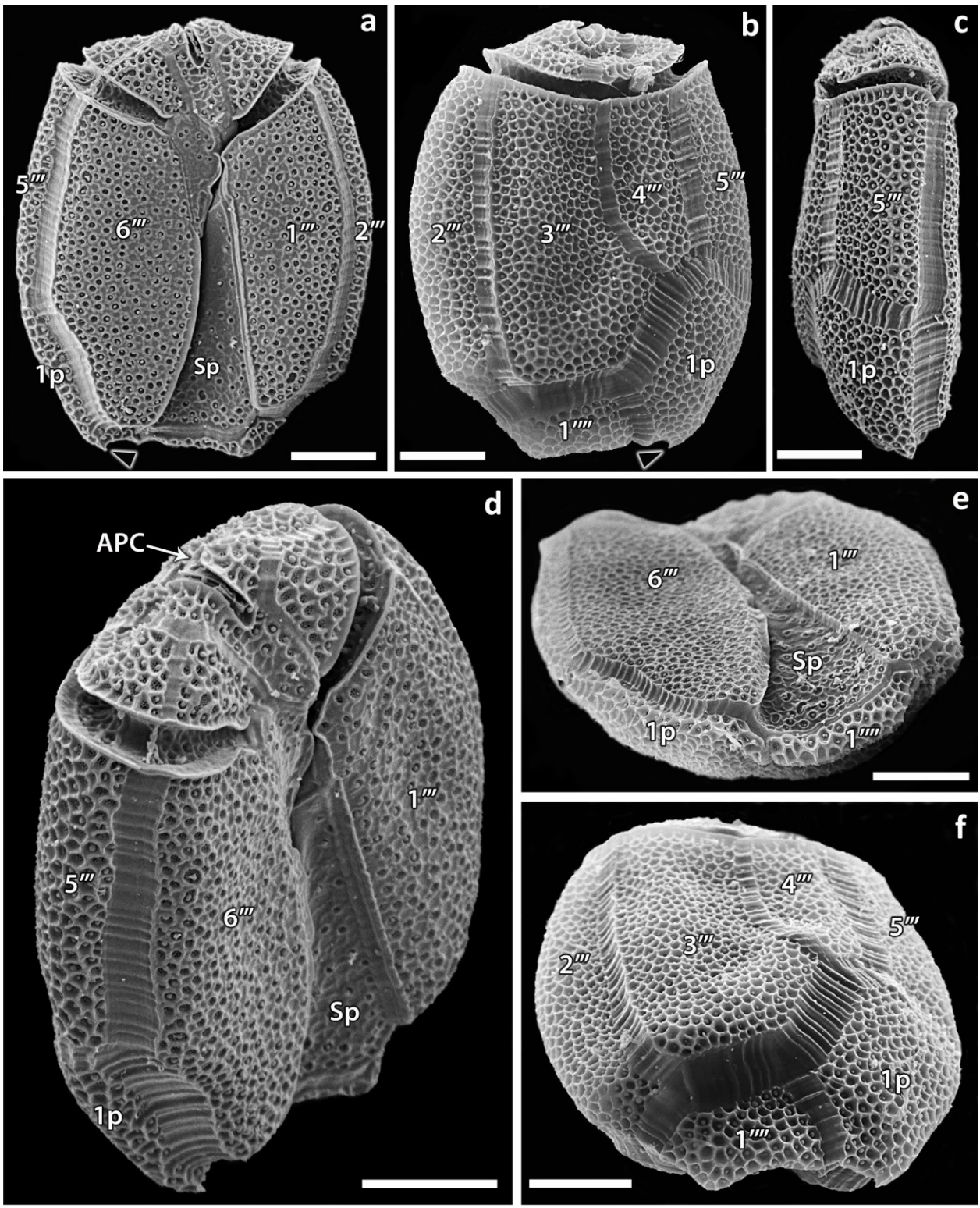

804 Fig. 3. Scanning electron micrographs of *Ailadinium reticulatum* gen. et sp. nov. (stub #
805 CEDiT2014H35; holotype specimen*). (a, b) Ventral (a) and dorsal (b) views. Arrowheads point
806 the antapical spine. (c) Right lateral view. (d) Oblique right lateral view. (e, f) Antapical views of
807 ventral (e) and dorsal (f) cell side. Scale bar, 10 μm.
808 * - the holotype specimen was found as attached to the stub surface with its antapex so that cell
809 was in a slightly oblique position allowing to obtain the ventral (a), right lateral (c, d) views, and
810 antapical view of ventral cell side (e). During re-examination of the same specimen, it was found
811 to be fallen to its ventral side due to the dorsal view (b) and antapical view of dorsal cell side (f)
812 were obtained from the same specimen.
813

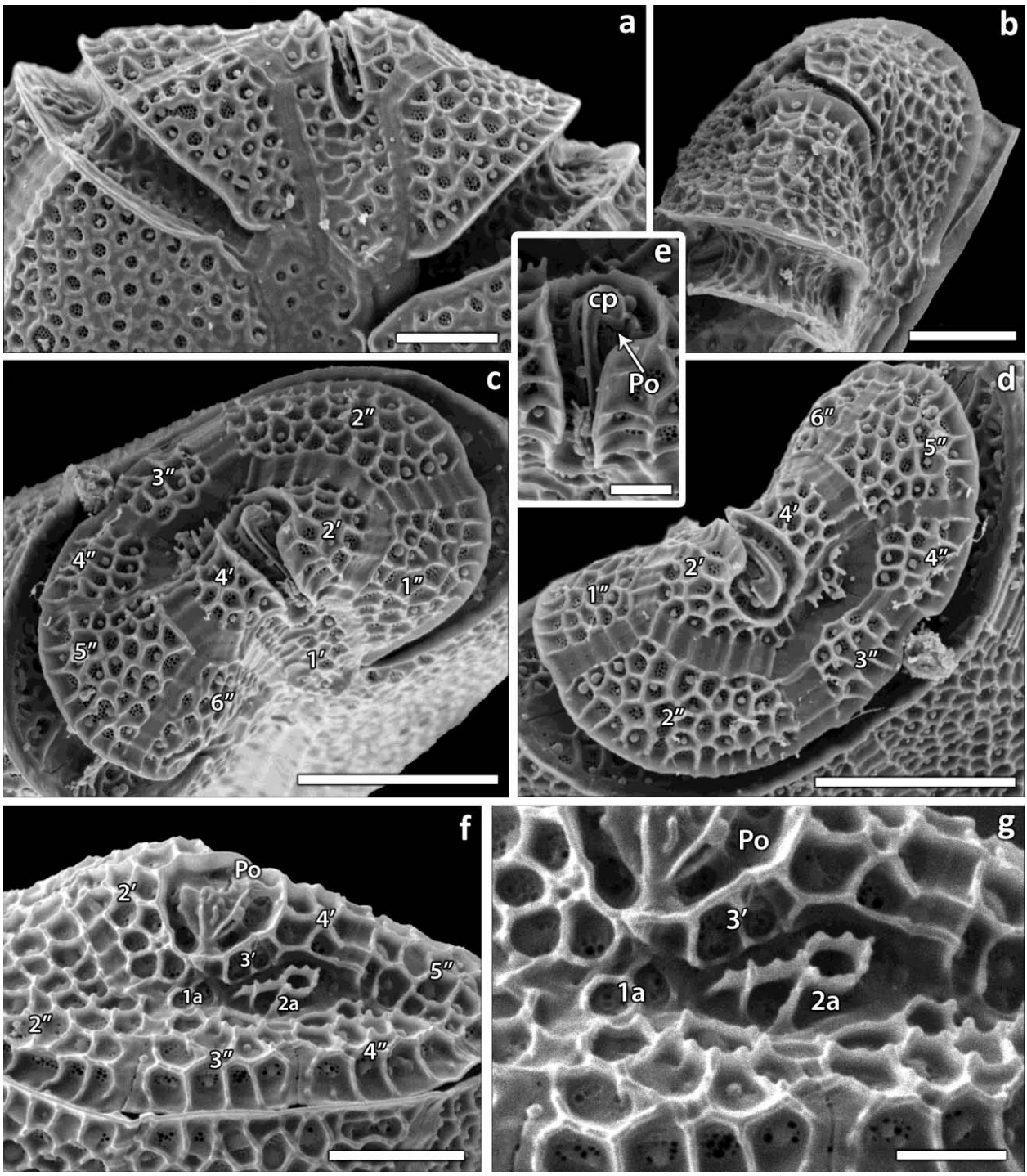

814

815 Fig. 4. Scanning electron micrographs of *Ailadinium reticulatum* gen. et sp. nov. (stub #
816 CEDiT2014H35). (a-g) Epitheca: (a) Ventral view. (b) Oblique right lateral view. (c, d) Apical
817 views showing the epithecal plate pattern. (e) Detail of the apical view of the epitheca showing
818 the APC. (f, g) Details of the dorsal side of the epitheca showing the plate pattern. Scale bars, 10
819 μm in (c, d), 5 μm in (a, b, f) and 2 μm in (e, g).
820

821

822

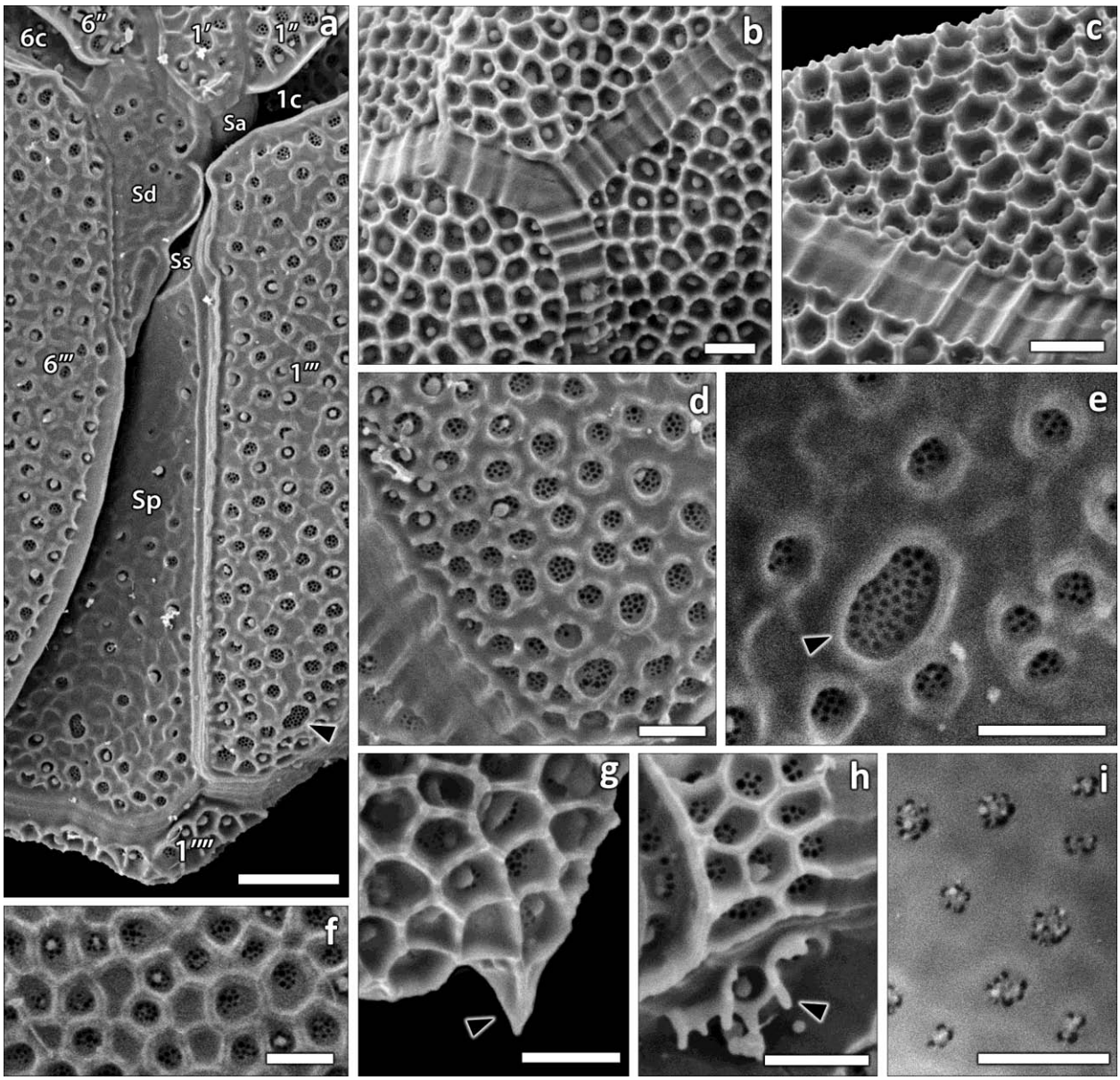

Fig. 5. Scanning electron micrographs of *Ailadinium reticulatum* gen. et sp. nov. (stub # CEDiT2014H35). (a) Detail of the ventral side of the hypotheca showing the sulcus and surrounded plates. Arrowhead points the large marginal depression with sieve-like bottom. (b) Detail of the dorsal side of the hypotheca showing reticulate thecal surface and sutures. (c) Detail of the dorsal side of the hypotheca in oblique view showing the polygonal depressions with well-developed raised and crenulated sides and sutures. (d) Detail of the ventral side of the hypotheca showing the foveate thecal ornamentation consisting of round depressions with small pores at the bottom. (e) Detail of the ventral side of the hypotheca showing the large marginal depression with sieve-like bottom (arrowhead) and incomplete ridges between depressions. (f) Detail of the dorsal side of the hypotheca showing the polygonal depressions with numerous small pores at the bottom and depressions without pores. (g) Detail of the antapical part of the dorsal side of the hypotheca showing the asymmetrical spine (arrowhead). (h) Detail of the dorsal side of the epitheca showing the 2a plate with depressions surrounded by crest-like rims. (i) Inside view of the depressions of ventral cell side. Scale bars, 5 μm in (a) and 2 μm in (b-i).

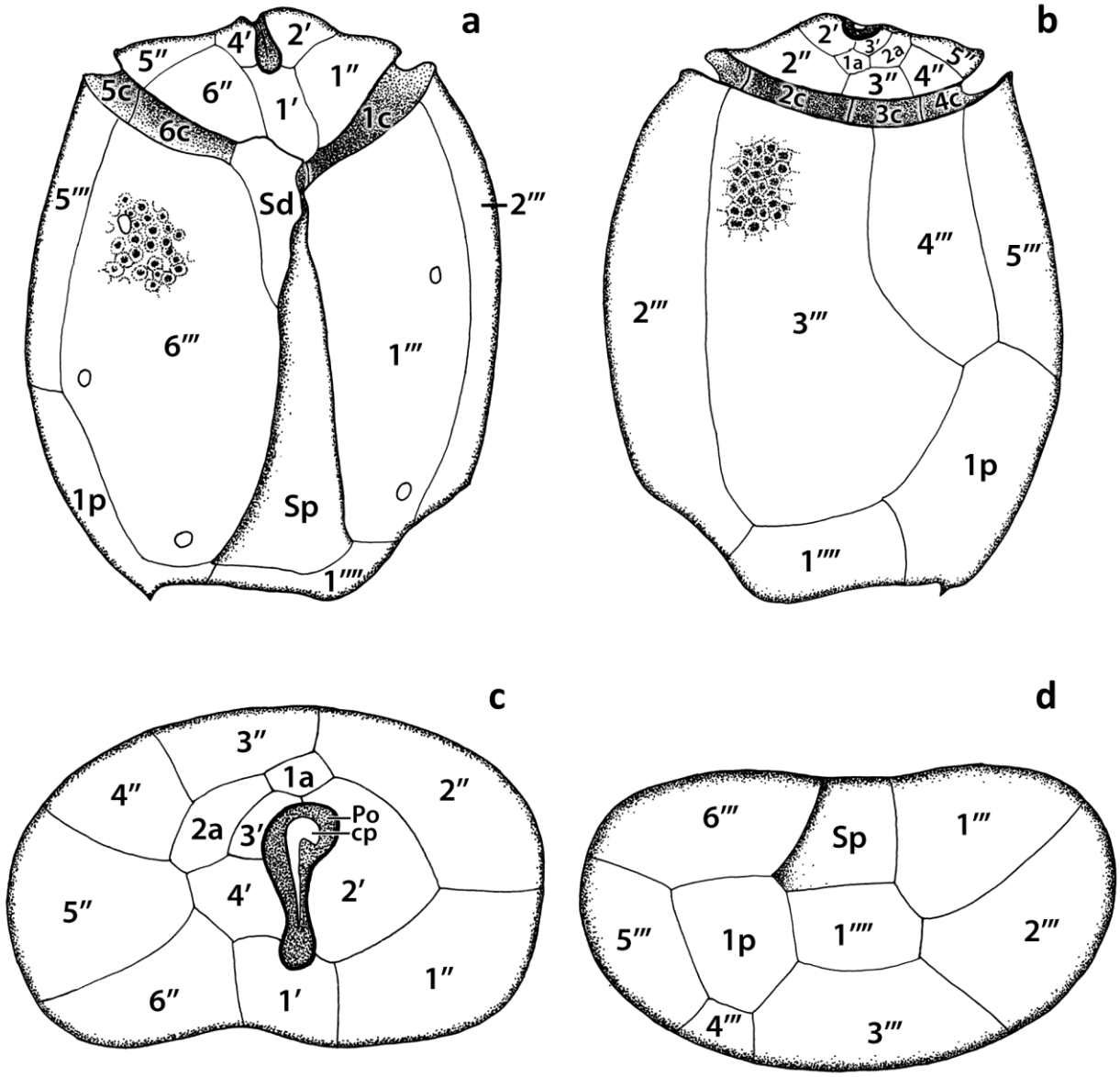

840

841 Fig. 6. Line drawings of *Ailadinium reticulatum* gen. et sp. nov. (a) Ventral view. (b) Dorsal
842 view. (c) Apical view. (d) Antapical view.
843

844

845

846

847

848

849

850

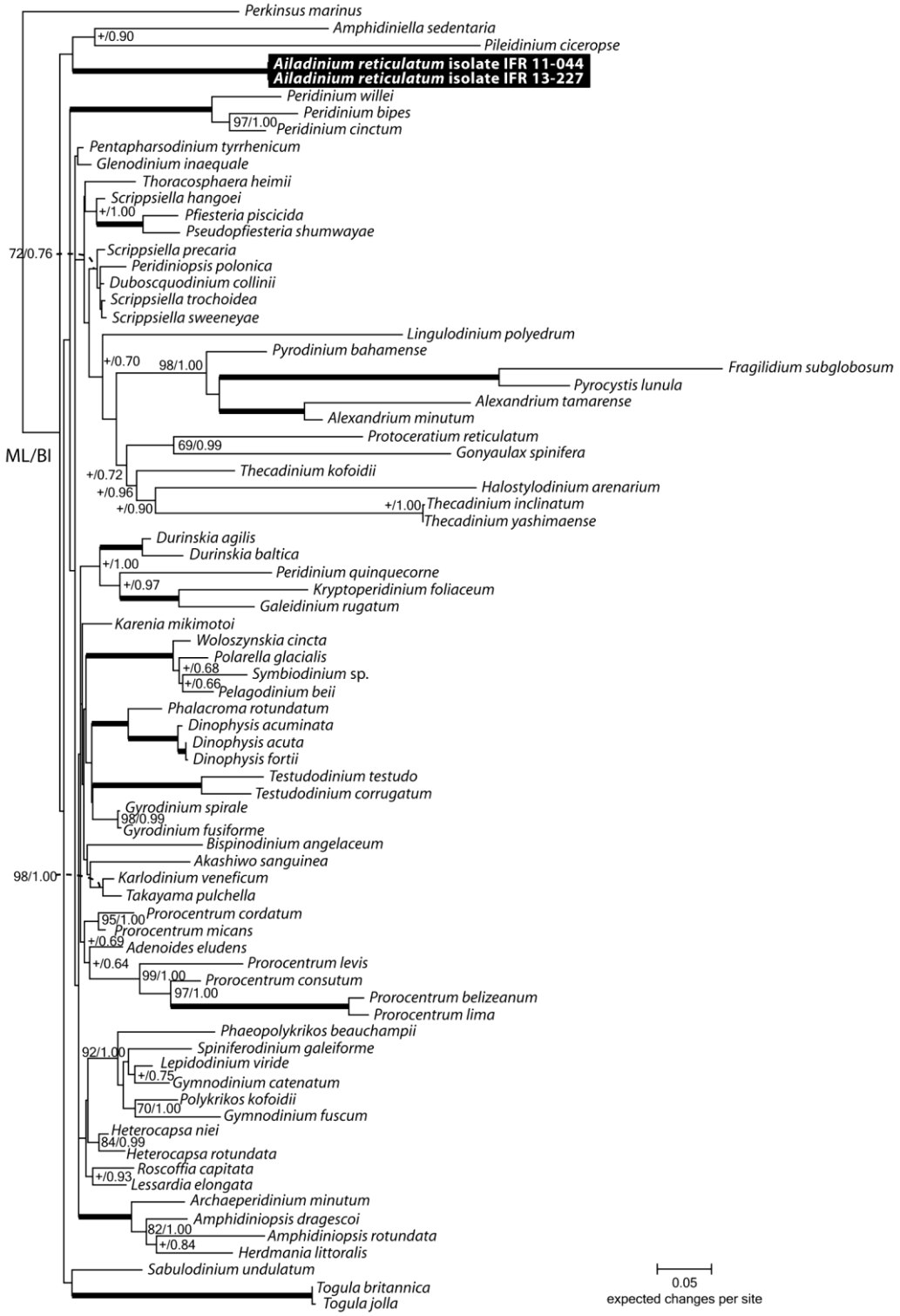

Fig. 7. Maximum likelihood (ML) phylogenetic tree inferred from SSU rDNA (matrix of 77 taxa and 1691 aligned positions). The tree was rooted using *Perkinsus marinus* sequence as outgroup. Model selected GTR + I + Γ_4. Log likelihood =-20365.9. Substitution rate matrix: A ↔ C = 1.554361, A ↔ G = 4.42400, A ↔ T = 1.43955, C ↔ G = 0.81454, C ↔ T = 9.29164, against G ↔ T = 1.00000. Assumed nucleotide frequencies: f(A)=0.24586, f(C)=0.19302, f(G)=0.25297, f(T)=0.30815. Among site rate variation: assumed proportion of invariable sites I = 0.324. Rates at variable site assumed to be gamma distributed with shape parameter α = 0.524. Bootstrap values (1,000 pseudoreplicates) > 65 (in ML) and posterior probabilities > 0.5 (in BI) are shown at nodes, thick lines indicate full support of the branch (100/1.00). '+' indicate nodes present but unsupported.

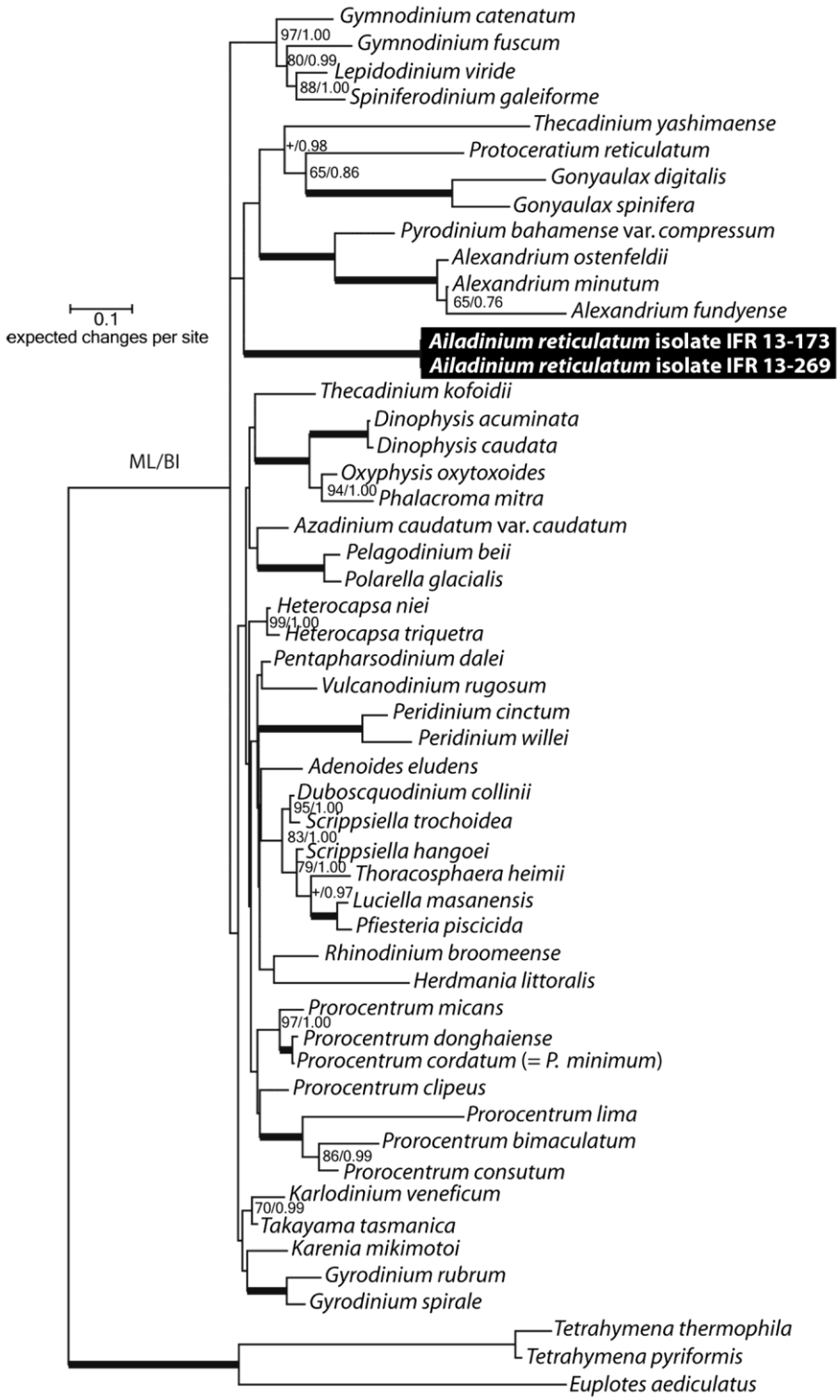

862 Fig. 8. Maximum likelihood (ML) phylogenetic tree inferred from partial LSU rDNA (matrix of
863 52 taxa and 812 aligned positions). The tree was rooted using sequences of the Ciliates *Euplotes*
864 *aediculatus*, *Tetrahymena pyriformis* and *Tetrahymena thermophila* as external group. Model
865 selected GTR + Γ_5. Log likelihood = -12325.47954. Substitution rate matrix: A ↔ C = 0.78972,
866 A ↔ G = 2.47397, A ↔ T = 0.93648, C ↔ G = 0.64402, C ↔ T = 6.36575, against G ↔ T =
867 1.00000. Assumed nucleotides frequencies f(A)=0.27083, f(C)=0.19006, f(G)=0.27936,
868 f(T)=0.25975. Rates at variable site assumed to be gamma distributed with shape parameter α =
869 0.466. Only bootstrap values (1,000 pseudoreplicates) > 65 (in ML) and posterior probabilities >
870 0.5 (in BI) are shown at nodes; thick lines indicate full support of the branch (100/1.00); '+'
871 indicates a node present but unsupported while absence of value indicate an unsupported branch
872 in ML and BI.

SUPPLEMENTARY MATERIAL

APPENDIX S1: List of sequences used in phylogenetic analyses

GenBank accession numbers (in bold, sequences acquired in this study):

SSU rDNA sequences:

Adenoides eludens AF274249; *Akashiwo sanguinea* U41085; *Alexandrium minutum* JF521634; *Alexandrium tamarense* AF022191; *Amphidiniella sedentaria* AB212091; *Amphidiniopsis* (as *Thecadinium*) *dragescoi* AY238479; *Amphidiniopsis rotundata* AB639343; *Archaeperidinium minutum* AB780999; *Bispinodinium angelaceum* AB762397; *Dinophysis acuminata* FJ869120; *Dinophysis acuta* AJ506973; *Dinophysis fortii* AB073118; *Duboscquodinium collinii* HM483399; *Durinskia agilis* JF514516; *Durinskia baltica* GU999528; *Fragilidium subglobosum* AF033869; *Galeidinium rugatum* AB195668; *Glenodinium inaequale* EF058237; *Gonyaulax spinifera* AF022155; *Gymnodinium catenatum* DQ779990; *Gymnodinium fuscum* AF022194; *Gyrodinium fusiforme* AB120002; *Gyrodinium spirale* AB120001; *Halostylodinium arenarium* AB036837; *Herdmania littoralis* AB564302; *Heterocapsa niei* EF492499; *Heterocapsa rotundata* DQ388464; *Karenia mikimotoi* AF009131; *Karlodinium veneficum* EF492506; *Kryptoperidinium foliaceum* EF492508; *Lepidodinium viride* DQ499645; *Lessardia elongata* AF521100; *Lingulodinium polyedrum* AB693196; *Pelagodinium beii* JF791066; *Pentapharsodinium tyrrhenicum* AF022201; *Peridiniopsis polonica* AY443017 ; *Peridinium bipes* AF231805; *Peridinium cinctum* EF058243; *Peridinium quinquecorne* AB246744; *Peridinium willei* EF058249; *Perkinsus marinus* AF126013; *Pfiesteria piscicida* DQ991382; *Phalacroma rotundatum* AJ506975; *Pheopolykrikos beauchampii* DQ371294; *Pileidinium ciceropse* AB211357; *Polarella glacialis* AF099183; *Polykrikos kofoidii* DQ371291; *Prorocentrum belizeanum* DQ238042; *Prorocentrum consutum* FJ842379; *Prorocentrum levis* DQ238043; *Prorocentrum lima* Y16235; *Prorocentrum micans* EU780638; *Prorocentrum*

minimum JX402086; *Protoceratium reticulatum* DQ217789; *Pseudopfiesteria shumwayae* AF080098; *Pyrocystis lunula* AF274274; *Pyrodinium bahamense* AF274275; ***Ailadinium reticulatum*** **isolate IFR 11-044 KJ187034;** ***Ailadinium reticulatum*** **isolate IFR 13-227 KJ187035**; *Roscoffia capitata* AF521101; *Sabulodinium undulatum* DQ975474; *Scippsiella sweeneyae* HQ845331; *Scrippsiella hangoei* EF417316; *Scrippsiella precaria* DQ847435; *Scrippsiella trochoidea* FR865630; *Spiniferodinium galeiforme* GU295203; *Symbiodinium* sp. AB085911; *Takayama xiamenensis* AY800130; *Testudodinium corrugatum* AB704004; *Testudodinium testudo* AB704002; *Thecadinium inclinatum* EF492515; *Thecadinium kofoidii* AY238478; *Thecadinium yashimaense* AY238477; *Thoracosphaera heimii* HQ845327; *Togula britannica* (as *Amphidinium brittanicum*) AY443010; *Togula jolla* (as *Amphidinium corpulentum*) AF274252; *Woloszynskia halophila* EF058252.

LSU rDNA sequences:

Adenoides eludens FJ939580; *Alexandrium fundyense* FJ411147; *Alexandrium minutum* JF521635; *Alexandrium ostenfeldii* EU707483; *Azadinium caudatum* var. *caudatum* JQ247702; *Dinophysis acuminata* EF613351; *Dinophysis caudata* EU780644; *Duboscquodinium collinii* HM483399; *Euplotes aediculatus* AF223571; *Gonyaulax digitalis* AY154963; *Gonyaulax spinifera* AY154960; *Gymnodinium catenatum* JQ616825; *Gymnodinium fuscum* AF200676; *Gyrodinium rubrum* AY571369; *Gyrodinium spirale* AY571371; *Herdmania littoralis* AB564306; *Heterocapsa niei* JQ247713; *Heterocapsa triquetra* HQ902268; *Karenia mikimotoi* EF469238; *Karlodinium veneficum* DQ114466; *Lepidodinium viride* DQ499645; *Luciella masanensis* EU048553; *Oxyphysis oxytoxoides* EF613359; *Pelagodinium beii* DQ195370; *Pentapharsodinium dalei* JX262498; *Peridinium cinctum* EF205011; *Peridinium willei* EF205012; *Pfiesteria piscicida* FJ600087; *Phalacroma mitra* FJ808706; *Polarella glacialis* JN558110; *Prorocentrum bimaculatum* HQ890883; *Prorocentrum clipeus* JX912175; *Prorocentrum consutum* FJ842378; *Prorocentrum cordatum* EU780639; *Prorocentrum*

925 *donghaiense* AY822610; *Prorocentrum lima* DQ336189; *Prorocentrum micans* X16108;
926 *Protoceratium reticulatum* AF260386; *Pyrodinium bahamense* var. *compressum* AY154959;
927 ***Ailadinium reticulatum* isolate IFR 13-173 KJ187036; *Ailadinium reticulatum* isolate IFR**
928 **13-269 KJ187037**; *Rhinodinium broomeense* DQ078782; *Scrippsiella hangoei* EF205016;
929 *Scrippsiella trochoidea* HQ670228; *Spiniferodinium galeiforme* GU295206; *Takayama*
930 *tasmanica* AY284948; *Tetrahymena pyriformis* X54004; *Tetrahymena thermophila* X54512;
931 *Thecadinium kofoidii* GU295207; *Thecadinium yashimaense* GU295209; *Thoracosphaera heimii*
932 EF205018; *Vulcanodinium rugosum* HQ622103.
933